NANO LETTERS

LETTER

pubs.acs.org/NanoLett

Studies of Intrinsic Hot Phonon Dynamics in Suspended Graphene by Transient Absorption Microscopy

Bo Gao,[†,‡] Gregory Hartland,[‡] Tian Fang,[§] Michelle Kelly,[§] Debdeep Jena,[§] Huili (Grace) Xing,[§] and Libai Huang*[,†]

[†]Notre Dame Radiation Laboratory, [‡]Department of Chemistry and Biochemistry, and [§]Department of Electrical Engineering, University of Notre Dame, Notre Dame, Indiana 46556, United States

Supporting Information

ABSTRACT: Correlated transient absorption and atomic force microscopy (AFM) measurements have been performed for monolayer graphene, both free-standing and supported on a glass substrate. The AFM images allow us to locate regions of the suspended graphene. The transient absorption traces show a fast instrument response limited decay, followed by a slower intensity dependent decay. The fast decay is assigned to a combination of coupling between the excited charge carriers and the optical phonon modes of graphene and the substrate, and diffusion of the charge carrier out of the probe region. The slow decay is due to the hot phonon effect and reflects the lifetime of the intrinsic optical phonons of graphene. The time constant for the slow decay is longer for suspended graphene compared to substrate-supported graphene. This is attributed to interactions between the excited charge carriers and the surface optical phonon modes of the substrate, which supplies an additional relaxation channel for supported graphene.

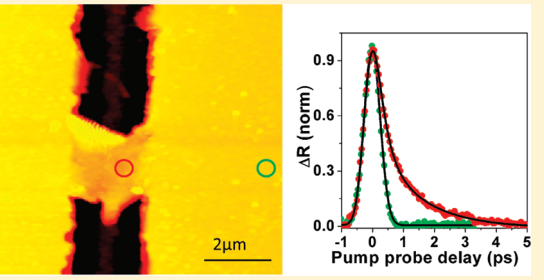

KEYWORDS: Graphene, transient absorption imaging, hot phonon effect, remote phonon scattering

Graphene is a two-dimensional material with a single atomic layer of carbon atoms arranged in a hexagonal lattice. The unique structure of graphene leads to many unusual physical properties, for example, linear energy dispersion near the Dirac point and near ballistic transport of charge carriers.[1,2] From a device standpoint, a low field mobility of up to 200 000 $cm^2 V^{-1} s^{-1}$ in graphene is extremely attractive for applications such as nanoscale field effect transistors and single-electron transistors.[3−6] One of the main mechanisms that limit charge transport in graphene is phonon scattering.[7,8] A thorough understanding of carrier-phonon interactions is thus important for realizing the full potential of graphene.

The dominant charge carrier cooling mechanism at high electronic temperature in graphene is emission of optical phonons.[9,10] At high carrier densities, the optical phonons have a much greater generation rate than relaxation rate, which leads to a significant population of hot (nonequilibrium) optical phonons.[11,12] When the hot charge carriers and the optical phonon modes reach a quasi-equilibrium, the relaxation of the optical phonons represents a bottleneck in carrier cooling and transport.[13] This is known as the hot phonon effect. The hot phonon effect is particularly relevant for high-field transport.[7] Ultrafast spectroscopy is a powerful tool for studying charge carrier and phonon dynamics in materials, and has been applied to study carrier-cooling mechanisms in graphene.[10,14−19] We have previously reported transient absorption studies of the hot phonon effect in both chemical vapor deposition (CVD) and epitaxially grown graphene.[18,20] The transient absorption traces show an instrument response limited fast decay, which was assigned to coupling between the electrons and optical phonons, and a slower, intensity dependent picosecond time scale decay due to the hot phonon effect.[18,20]

For epitaxial graphene, measurements performed with diffraction-limited resolution show significant spatial heterogeneity in the slow decay. This was attributed to differences in coupling between graphene and the substrate.[18,20] One way this can occur for graphene on polar substrates is through remote charge carrier scattering by surface optical phonon modes (SOPs) of the substrate.[21] The SOPs provides an additional cooling pathway that reduces the hot phonon effect.[8,21] The majority of ultrafast studies of charge carrier-phonon interactions in graphene have been carried out with substrate-supported graphene, where intrinsic carrier-phonon scattering is convoluted with remote scattering by SOPs. This makes it difficult to separate the effects of the intrinsic optical phonons (IOPs) of graphene from that of SOPs. Understanding the dynamics of the IOPs is important for optimizing device performance. For example, recent Monte Carlo simulations predict that the hot phonon effect from the IOPs is the dominant contribution in current saturation for graphene at high-fields.[7]

In this Letter, the effect of the IOPs on charge carrier cooling and hot phonon dynamics is separated from the SOPs by comparing monolayer graphene suspended over micrometer-sized trenches to supported graphene on a glass substrate. By

Received: April 26, 2011
Revised: June 10, 2011
Published: June 22, 2011

combining our ultrafast transient absorption microscopy instrument with an atomic force microscope (AFM), we were able to locate suspended graphene and interrogate the charge-carrier dynamics with a temporal resolution of ~300 fs and a spatial resolution of ~200 nm. We observed remarkably different hot phonon dynamics for suspended and substrate-supported graphene. At sufficiently high excitation intensities, accumulation of the IOPs gives rise to the hot phonon effect for both suspended and substrate-supported graphene. However, at a given excitation energy, the phonon population is much higher for suspended graphene than for substrate-supported graphene, due to additional cooling channels provided by the SOPs of the substrate. The relaxation times measured at high excitation fluences in these experiments reflect the optical phonon lifetimes of the sample. We observed an optical phonon lifetime of 1.2 ± 0.1 ps for substrate-supported graphene that agrees well with recent time-resolved Raman measurements.[12] The optical phonon lifetime for suspended graphene is longer 1.8 ± 0.1 ps and is close to the value for graphite.[11] Our results show that the substrate plays an important role in the charge carrier and phonon dynamics for graphene.

Pristine graphene was grown on 25 μm thick copper foil in a low-pressure CVD system, which has been shown to give large area, single layer graphene.[22] Trenches of 2 μm wide and 0.35 μm deep were fabricated on a glass substrate by photolithography and reactive ion etching. In order to transfer graphene onto the glass substrate, a polymethyl methacrylate (PMMA, MW = 950 K) solution in chlorobenzene (4 wt %) was spin-casted on top of graphene on copper foil at 3000 rpm for 1 min and then baked at 170 °C for 1 h to form a 250 nm thick film. The copper foil was etched away by immersing in a ferric chloride aqueous solution (30 wt %). After rinsing with deionized water, the graphene-PMMA film was transferred onto the fabricated glass slide. The glass slide with graphene and the PMMA film on top was then annealed at 420 °C for 30 min under Ar/H_2 atmosphere to decompose the PMMA.

Correlated transient absorption microscopy/AFM measurements were performed by coupling a Ti/Sapphire oscillator (76 MHz repetition rate, Coherent Mira 900) with a Veeco Bioscope II AFM (operated in tapping mode for height imaging) mounted on an inverted microscope (Nikon Ti−U). A schematic of the experimental setup is shown in Figure 1a. For more details, please also see Figure S1 of the Supporting Information. The output from the Ti/Sapphire oscillator at 800 nm was split into two beams, one of which is doubled by a 0.4 mm thick β-barium borate crystal to provide the pump pulses. The polarizations of the pump and probe beams were made parallel, and the beams were focused at the sample with a 60×, 1.49 numerical aperture (NA) oil-immersion objective (Nikon Apo TIRF). In all the measurements described below, the pump and probe beams were spatially overlapped at the sample. The reflected beams were collected by the same objective, and the probe was detected with an avalanche photodiode (APD, Hamamatsu C5331−12). Pump-induced changes in the probe reflectance (ΔR) were measured by modulating the pump beam at 100 kHz with an acousto-optic modulator (AOM, IntraAction Corp, AOM-40AF Series) and monitoring the output of the APD with a lock-in amplifier (Stanford Research Systems, SR830). Transient absorption traces were obtained by delaying the probe with respect to the pump with a mechanical translation stage (Newport Corp.). The time-resolution at the sample was ca. 300 fs. Transient absorption images at a fixed pump−probe delay were acquired by raster scanning the sample with the Veeco Bioscope II software and recording the change in reflectivity of the probe ΔR. The spot size of the pump at the sample is ~200 nm and the spot size of the probe is ~400 nm, giving an overall spatial resolution of ~200 nm in these images. Raman spectra were collected by a Renishaw Raman microscope (RM1000) equipped with an argon-ion laser at 514 nm as an excitation source. The excitation beam was focused by a 50×, 0.75NA objective to a ~0.5 μm spot size, and the Raman scattered light was collected with the same objective.

Figure 1a shows a schematic of the experimental configuration. Figure 1b shows a tapping mode AFM image of the topography of the graphene sample. As indicated by the black dotted square in Figure 1b, there is a $\sim 2 \times 2$ μm^2 piece of graphene suspending across a trench (trench dimensions 2 μm wide and 0.35 μm deep). The suspended graphene droops across the trench, as shown by the AFM cross section in Figure 1c. The cross-section measurements show that graphene is sufficiently high above the bottom of the trench to be considered as freely suspended in air. There are two smaller pieces of graphene suspended on the edge of the trench as indicated by the white dotted squares at the top of the image in Figure 1b. These pieces are not large enough to cover the trench. Raman measurements (Figure S2 in Supporting Information) confirm that both the suspended and supported graphene are monolayers. Suspending graphene over a trench could introduce mechanical strain. At very low laser power, where heating effects can be excluded, Raman measurements show a G-band frequency of 1578 cm^{-1}, which is 2 cm^{-1} downshifted from the neutral position of 1580 cm^{-1} (Figure S2 in Supporting Information). Previous experiments have shown that a 1% strain in graphene produces a G band frequency downshift of 60 cm^{-1}.[23] This indicates that the strain in the suspended graphene is only 0.03%, which is negligible. The Raman measurements also show that the graphene completely covers the substrate, that is, there is graphene at the bottom of the trench in regions where no suspended graphene is evident. These pieces are not large enough to span the trench and simply fall to the bottom during the transfer process.

The absorption of the probe beam by graphene is proportional to $f_v(1 - f_c)$, where f_v and f_c are the Fermi−Dirac distribution functions for the valence and conduction band, respectively.[14] Thus, the 800 nm (1.55 eV) probe pulse in our transient absorption experiments monitors the change in the high-energy tail of the Fermi distribution as a function of time. Figure 1d,e shows transient absorption images recorded at 0 and 1.25 ps pump−probe delay, respectively, of the same region of the sample as the AFM image in Figure 1b. Almost the whole area imaged has a strong transient absorption signal at 0 ps delay, indicating that the area is covered by graphene, which is in accordance with the Raman measurements. The suspended graphene areas (the dotted squares in Figure 1d) have stronger signals than the substrate-supported graphene due to higher overall reflectivity (note that the transient absorption images plot ΔR not $\Delta R/R$). This is consistent with a stronger Raman signal for the suspended graphene areas (Figure S2 in Supporting Information). At 1.25 ps delay there is almost no signal from substrate-supported graphene, indicating that most of the charge carriers have relaxed outside the detection bandwidth of the probe pulses. In contrast, suspended graphene still has a significant transient absorption signal at 1.25 ps pump−probe delay, suggesting much slower carrier cooling.

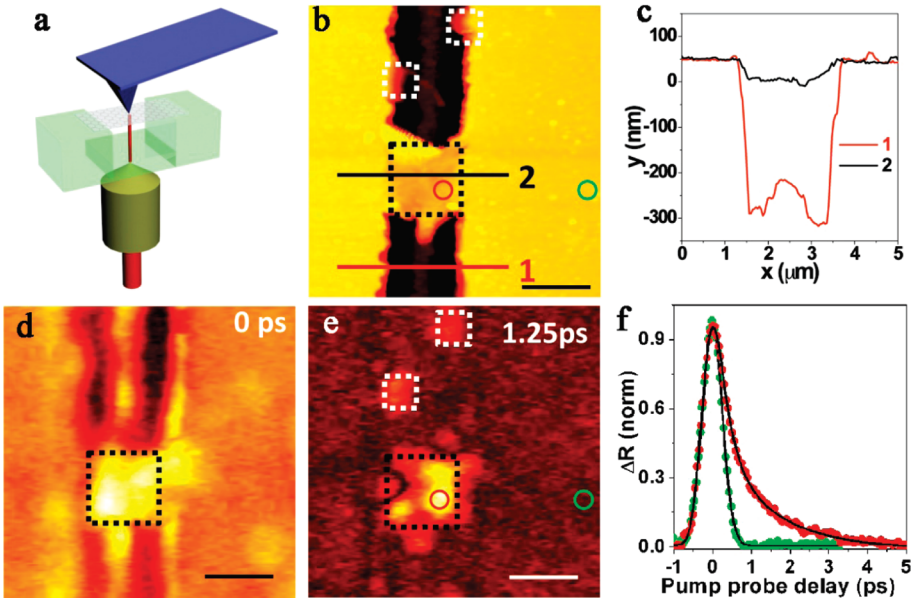

Figure 1. (a) Schematic that shows the combined AFM-transient absorption microscopy measurements. (b) AFM height image of the graphene sample. (c) Line profile taken along the lines indicated in b. (d) Transient absorption image of the same area at 0 ps delay. (e) Transient absorption image at 1.25 ps delay. (f) Transient absorption traces collected for suspended graphene (red filled circles) and substrate-supported graphene (green filled circles). The positions where the kinetics is collected are indicated by the red and green circles in b and e. The scale bars in b,d,e are 2 μm. The pump fluence was 2 mJ/cm^2 for these measurements.

The difference in carrier cooling dynamics is more clearly displayed in Figure 1f, where transient absorption traces are compared for suspended (red circle in Figure 1b,e) and substrate-supported graphene (green circle in Figures 1b and 1e) at a pump laser fluence of 2 mJ/cm^2. The decay dynamics for substrate-supported graphene at this laser fluence is instrumental limited, which is consistent with the ultrafast ~200 fs time scale electron−phonon coupling.[24] The dynamics for suspended graphene, on the other hand, has an additional slow decay component. By fitting the decay curve with a biexponential decay convoluted with a Gaussian response function, we found a instrumental limited fast decay and a slow decay of 1.4 ± 0.1 ps for the suspended graphene. The slow decay component was attributed to the hot phonon effect in our previous studies.[18,20] The present results show that accumulation of hot phonons occurs more readily in suspended graphene than substrate supported graphene. Similar results were observed in another suspended graphene sample (Figure S3 in Supporting Information).

Note that because the pieces of suspended graphene have relatively small dimensions in our samples, a high NA objective is needed for these measurements. This creates a small laser spot size at the sample, which means that charge carrier diffusion is a significant issue in our transient absorption experiments.[25] Using the diffusion constants measured in ref 25, we estimate that ~95% of the carriers diffuse out of the probe region within 0.5 ps. This has several consequences. First, we need to use much higher pump powers to generate a signal compared to studies performed at lower magnification. Second, the charge carrier diffusion makes it very hard to quantify the temperature in the experiments. Thus, for the ultrafast measurements below we report the incident pump fluence and do not try and determine the electron or phonon temperatures.

The effect of carrier diffusion on the dynamics (not the main focus of this paper) was examined by varying the size of the pump and probe beams, and comparing transient absorption traces recorded at equivalent pump laser fluences (Figure S4 in Supporting Information). At low pump fluences, we observe differences in the form of the transient absorption traces for experiments performed with high and low NA objectives. Specifically, the relative magnitude of the fast decay to the signal is much larger for a smaller laser spot size. This indicates that carrier diffusion makes a significant contribution to the fast decay in experiments performed with the high NA objective. However, the time scale for the slow decay in the transient absorption traces is the same for the high and low NA experiments. Indeed, at high pump fluences, where the slow decay dominates the dynamics, the transient absorption traces do not change significantly when we vary the spot size. The slow decay is assigned to the relaxation of the optical phonons created by carrier cooling. These phonons diffuse on a much slower time scale than the electrons, so that their relaxation time constant is not sensitive to the laser spot size.

In order to characterize the hot phonon effect in suspended graphene and understand the role of the substrate, we performed pump intensity dependence studies for both suspended and substrate-supported graphene. The results are shown in Figure 2. For both areas, a linear relationship between the magnitude of the transient absorption signal at zero time delay and pump power was observed (data not shown), which implies that we do not saturate the optical transitions in these experiments. The pump laser fluence was varied from 0.3 to 5 mJ/cm^2 for suspended graphene, and 1.7−35 mJ/cm^2 for substrate-supported graphene. A pump fluence of 1 mJ/cm^2 corresponds to an initial carrier density of ~4 × 10^{13} cm^{-2} per graphene layer. Note that pump laser fluences larger than 5 mJ/cm^2 damage the suspended graphene.

For substrate-supported graphene (Figure 2a), at low pump intensity (up to a pump fluence of 3 mJ/cm^2) the carrier

dx.doi.org/10.1021/nl201397a |*Nano Lett.* 2011, 11, 3184–3189

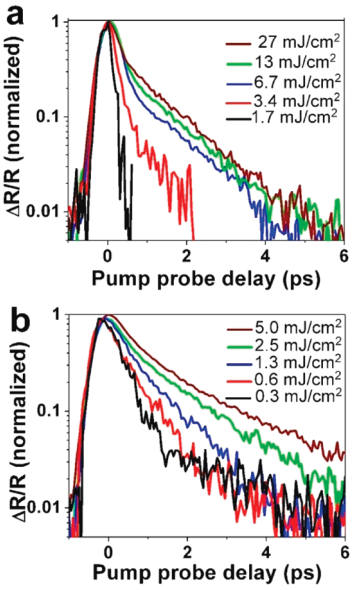

Figure 2. (a) Transient absorption traces at different incident pump intensities for substrate-supported graphene (green circle in Figure 1e). (b) Data for suspended graphene (red circle in Figure 1e). The traces are normalized by the maximum signal intensity.

dynamics exhibit an instrument-limited decay (time constant τ_1 < 0.2 ps). As the pump fluence increases, a second and slower decay component τ_2 appears that accounts for 20−40% of the total signal. The value of τ_2 is plotted against pump fluence in Figure 3. The slow time-constant for substrate-supported graphene reaches a constant value of 1.2 ± 0.1 ps at pump fluences greater than 13 mJ/cm^2. This value is identical to the G mode optical phonon lifetime of 1.2 ± 0.1 ps measured by time-resolved Raman experiments for monolayer graphene on SiO_2.[12] This is consistent with the slow decay arising from the hot phonon effect; at high carrier densities, the charge carrier relaxation is controlled by the lifetime of the strongly coupled intrinsic optical phonons.[13]

For suspended graphene, there are two notable differences in the carrier cooling dynamics in comparison to substrate-supported graphene. First, even at a low pump fluence of 0.3 mJ/cm^2, the carrier cooling is biexponential with a slow decay constant of τ_2 = 1.0 ± 0.1 ps. For a given pump laser fluence, the value of τ_2 is much larger for suspended graphene compared to supported graphene. At the highest pump fluence, we could use for suspended graphene τ_2 = 1.8 ± 0.1 ps, which is close to the optical phonon lifetime of 2.2 ± 0.1 ps measured for graphite.[11]

The difference in the τ_2 values for suspended and substrate-supported graphene indicates that the substrate plays an important role in relaxation of the optical phonons. The substrate can contribute additional cooling channels for hot carriers through coupling of the charge carriers to the SOPs of the substrate.[12,21,26,27] Fratini and Guinea showed that for SiO_2 substrates scattering of electrons in graphene by SOPs of the substrate (remote electron−phonon coupling) has a comparable rate to that for scattering by the IOPs modes of graphene.[21] The scattering rates for different phonon modes calculated as a function of electron energy are shown in Figure S5 in the Supporting Information. Interaction between the charge carriers of graphene and SOPs of the substrate has two effects. First, fewer IOPs are created for substrate-supported graphene compared to suspended graphene at a given

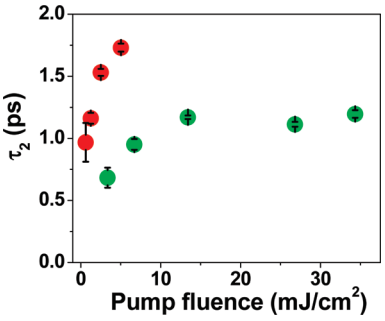

Figure 3. Slow decay constant τ_2 plotted as a function of the pump fluence for suspended graphene (red circles) and substrate-supported graphene (green circles). The time constants were obtained by fitting the transient absorption data in Figure 2 to a biexponential decay convoluted with a Gaussian instrument response.

excitation intensity. This explains the higher threshold intensity for the hot phonon effect in substrate-supported graphene (less IOPs are created for a given excitation level). The relaxation channel created by interaction between the charge carriers and the SOPs also reduces the lifetime of the IOPs of graphene.[11] In principle, phonon−phonon interactions between graphene and the substrate could also shorten the lifetime of the IOPs for substrate-supported graphene. Our measurements cannot differentiate between the two mechanisms. However, theoretical calculations predict that remote electron scattering by SOPs dominates the interaction between the graphene and the substrate.[21] Therefore, it is most likely that the reduction in the IOP lifetime from 1.8 ps for suspended graphene to 1.2 ps for substate-supported graphene is due to the remote electron scattering and not phonon−phonon interactions.

Another effect to be considered is doping of graphene by the substrate. Suspended graphene is generally undoped, and has much higher electrical mobility compared to supported graphene.[3,4] Graphene on glass is p-doped with an excess population of holes, which results in down shifting of the Fermi level. Raman spectroscopy was utilized to monitor the level of doping and shifting of the Fermi level in our samples.[28] The Raman spectra of the suspended and substrate-supported graphene are shown in Figure 4. We observed an upshifted and narrower Raman G band for substrate-supported graphene, consistent with a high doping level. The G band frequency for substrate-supported graphene is 1600 cm^{-1}, corresponding to a 0.4 eV downshifting of the Fermi level.[28] The G band for suspended graphene is ∼1580 cm^{-1} suggesting that it is undoped and the Fermi level is close to the Dirac point. The 0.4 eV shift of Fermi level is much smaller than the pump or probe pulse energies and, therefore, should not affect the charge carrier generation or probing processes. However, doping reduces the coupling between the charge carriers and the SOPs in single layer graphene as calculated by Fratini and Guinea.[21] At a Fermi level of 0.6 eV and an electron energy of 1 eV, the remote electron scattering rate by SOPs is 10 times slower for doped graphene compared to that of undoped graphene. This implies that if we could produce undoped supported graphene, the effect of the substrate on the intrinsic optical phonon lifetime would be even stronger than that observed in Figure.3.

In order to confirm accumulation of hot intrinsic optical phonons in graphene, Stokes and anti-Stokes Raman spectra of the G mode were collected for both substrate-supported and

dx.doi.org/10.1021/nl201397a |Nano Lett. 2011, 11, 3184–3189

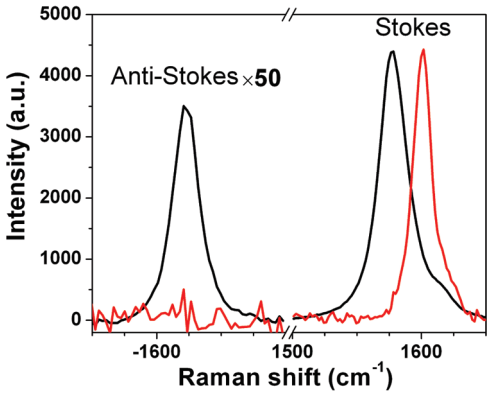

Figure 4. Stokes and anti-Stokes Raman spectra of the G band for suspended (black) and substrate-supported graphene (red). The excitation wavelength is 514 nm and the excitation power is 4.63 mW.

suspended graphene (Figure 4) at the same excitation intensity. The ratio between the anti-Stokes and Stokes signals is related to the optical phonon population and is given by

$$\frac{I_{AS}}{I_S} = exp\left(-\frac{\hbar\omega_G}{kT_G}\right) = \frac{n_G}{1+n_G} \approx n_G (n_G \ll 1)$$

where I_{AS} and I_S are the strength of anti-Stokes and Stokes G band signals, ω_G is the G mode optical phonon frequency, T_G is the effective optical phonon temperature, and n_G is the optical phonon occupation.[11] As shown in Figure 4, suspended graphene shows a substantial anti-Stokes signal while the substrate-supported graphene shows no significant anti-Stokes signal (note that the Stokes intensities are normalized). From the data presented in Figure 4, we deduce a phonon occupation of n_G of 0.016 for the suspended graphene at this excitation intensity. The anti-Stokes signal strength for substrate-supported graphene is at least 100 fold weaker than that of suspended graphene, suggesting a n_G value at least 100 times smaller. This observation directly demonstrates a larger population of intrinsic hot optical phonons in suspended graphene than in substrate-supported graphene at a given excitation intensity, which is consistent with the transient absorption data presented in Figures 1−3.

In conclusion, we have applied transient absorption microscopy combined with AFM imaging and Raman spectroscopy to study the intrinsic optical phonon dynamics in suspended graphene. We observed that the hot phonon effect occurs at much lower excitation intensity for suspended graphene compared to substrate-supported graphene. The lifetime of the IOPs created by charge carrier relaxation is also longer for suspended graphene compared to substrate-supported graphene. We attributed these observations to additional cooling channels provided by coupling between the charge carriers of graphene and SOPs of the substrate. These results show the importance of the environment in controlling the properties of graphene.

■ ASSOCIATED CONTENT

Supporting Information. Additional figures. This material is available free of charge via the Internet at http://pubs.acs.org.

■ AUTHOR INFORMATION

Corresponding Author
*E-mail: lhuang2@nd.edu.

■ ACKNOWLEDGMENT

L.H. and B.G. acknowledge the support from the Office of Basic Energy Science of the U.S. Department of the Energy (DE-FC02-04ER15533). G.H. and B.G. acknowledge the support from National Science Foundation (CHE-0647444). H.G.X. acknowledges the support from National Science Foundation (CAREER award). D.J., H.G.X. and M.K. acknowledge the support from National Science Foundation (ECCS-0802125), the Midwest Institute of Nanoelectronics Discovery (MIND), and the Center for Nanoscience and Technology at the University of Notre Dame. This is contribution No. NDRL 4883 from the Notre Dame Radiation Laboratory.

■ REFERENCES

(1) Novoselov, K.; Geim, A.; Morozov, S.; Jiang, D. *Science* **2004**, *306*, 666.
(2) Novoselov, K.; Geim, A.; Morozov, S.; Jiang, D. *Nature* **2005**, *438*, 197.
(3) Du, X.; Skachko, I.; Barker, A.; Andrei, E. Y. *Nat. Nanotechnol.* **2008**, *3*, 491.
(4) Bolotin, K. I.; Sikes, K. J.; Hone, J.; Stormer, H. L.; Kim, P. *Phys. Rev. Lett.* **2008**, *101*, 096802.
(5) Wang, F.; Zhang, Y.; Tian, C.; Girit, C. O.; Zettl, A. *Science* **2008**, *320*, 206.
(6) Avouris, P.; Chen, Z.; Perebeinos, V. *Nat. Nanotechnol.* **2007**, *2*, 605.
(7) Fang, T.; Konar, A.; Xing, H.; Jena, D. Arxiv preprint arXiv1008.1161v1.
(8) Meric, I.; Han, M. Y.; Young, A. F.; Ozyilmaz, B.; Kim, P.; Shepard, K. L. *Nat. Nanotechnol.* **2008**, *3*, 654.
(9) Suzuura, H.; Ando, T. *J. Phys.: Conf. Ser.* **2009**, *150*, 022080.
(10) Wang, H.; Strait, J.; George, P.; Shivaraman, S. *Appl. Phys. Lett.* **2010**, *96*, 081917.
(11) Yan, H.; Song, D.; Mak, K. F.; Chatzakis, I.; Maultzsch, J.; Heinz, T. F. *Phys. Rev. B* **2009**, *80*, 121403.
(12) Kang, K.; Abdula, D.; Cahill, D. G.; Shim, M. *Phys. Rev. B* **2010**, *81*, 165405.
(13) Shah, J. *Ultrafast spectroscopy of semiconductors and semiconductor nanostructures*: Springer: New York, 1999.
(14) Sun, D.; Wu, Z. K.; Divin, C.; Li, X. B.; Berger, C.; de Heer, W. A.; First, P. N.; Norris, T. B. *Phys. Rev. Lett.* **2008**, *101*, 157402.
(15) Choi, H.; Borondics, F.; Siegel, D. A.; Zhou, S. Y.; Martin, M. C.; Lanzara, A.; Kaindl, R. A. *Appl. Phys. Lett.* **2009**, *94*, 172102.
(16) Dawlaty, J. M.; Shivaraman, S.; Chandrashekhar, M.; Rana, F.; Spencer, M. G. *Appl. Phys. Lett.* **2008**, *92*, 042116.
(17) George, P. A.; Strait, J.; Dawlaty, J.; Shivaraman, S.; Chandrashekhar, M.; Rana, F.; Spencer, M. G. *Nano Lett.* **2008**, *8*, 4248.
(18) Huang, L. B.; Hartland, G. V.; Chu, L. Q.; Luxmi; Feenstra, R. M.; Lian, C. X.; Tahy, K.; Xing, H. L. *Nano Lett.* **2010**, *10*, 1308.
(19) Newson, R. W.; Dean, J.; Schmidt, B.; van Driel, H. M. *Opt. Express* **2009**, *17*, 2326.
(20) Huang, L.; Gao, B.; Hartland, G.; Kelly, M.; Xing, H. L. *Surf. Sci.* **2011**10.1016/j.susc.2010.12.009.
(21) Fratini, S.; Guinea, F. *Phys. Rev. B* **2008**, *77*, 195415.
(22) Li, X.; Cai, W.; An, J.; Kim, S.; Nah, J.; Yang, D. *Science* **2009**, *324*, 1312.
(23) Ding, F.; Ji, H.; Chen, Y.; Herklotz, A.; Doerr, K.; Mei, Y.; Rastelli, A.; Schmidt, O. G. *Nano Lett.* **2010**, *10*, 3453.

(24) Breusing, M.; Ropers, C.; Elsaesser, T. *Phys. Rev. Lett.* **2009**, *102*, 086809.
(25) Ruzicka, B.; Wang, S.; Werake, L.; Weintrub, B.; Loh, K.; Zhao, H. *Phys. Rev. B* **2010**, *82*, 195414.
(26) Viljas, J. K.; Heikkila, T. T. *Phys. Rev. B* **2010**, *81*, 245404.
(27) Petrov, A. G.; Rotkin, S. V. *JETP Lett.* **2006**, *84*, 156.
(28) Das, A.; Pisana, S.; Chakraborty, B.; Piscanec, S.; Saha, S. K.; Waghmare, U. V.; Novoselov, K. S.; Krishnamurthy, H. R.; Geim, A. K.; Ferrari, A. C.; Sood, A. K. *Nat. Nanotechnol.* **2008**, *3*, 210.